

# Dynamically Compensated Cams for Rigid Cam-Follower Systems with Fluctuating Cam Speed and Dominating Inertial Forces

B. Demeulenaere and J. De Schutter

K.U. Leuven, Department of Mechanical Engineering, Division P.M.A.  
Celestijnenlaan 300B, 3001 Heverlee, Belgium  
bram.demeulenaere@mech.kuleuven.ac.be  
<http://www.mech.kuleuven.ac.be>

*Abstract*— Traditionally, cam-follower systems are designed by assuming a constant camshaft speed. Nevertheless, all cam-follower systems, especially high-speed systems, exhibit some camshaft speed fluctuation (despite the presence of a flywheel) which causes the follower motions to be inaccurate. This paper therefore proposes a novel design procedure that explicitly takes into account the camshaft speed variation. The design procedure assumes that (i) the cam-follower system is conservative and (ii) all forces are inertial. The design procedure is based on a single design choice, i.e. the range of camshaft speed variation, and yields (i) cams that compensate for the inertial dynamics for any period of motion and (ii) a camshaft flywheel whose (small) inertia is independent of the period of motion. A design example shows that the cams designed in this way offer the following advantages, even for non-conservative, non-purely inertial cam-follower systems: (i) smaller flywheel, (ii) more accurate follower motions, (iii) lower motor torques and (iv) a camshaft motion spectrum that is easily and robustly predictable.

## I. INTRODUCTION

Methods for cam design have become increasingly sophisticated over the past several decades. Recent methods focus on the design of dynamically compensated cams with the purpose of minimizing residual vibrations in high-speed cam-follower systems. Srinivasan and Jeffrey Ge [15] distinguish three groups of methods: (i) the traditional polydyne method [16], [2] and more robust modifications of it [8], [15], (ii) numerical methods such as linear programming and quadratic optimization [10] and Lagrange multiplier techniques [19], [3] and (iii) methods based on optimal control theory<sup>1</sup> [4], [6].

All these methods only consider the dynamics of the cam follower and assume the angular speed of the cam to be constant. In practice, however, the angular speed is variable due to [9]: (i) variations in the angular velocity of the driving actuator due to load variations, (ii) backlash in the reduction gear between the actuator and the cam and (iii) wind-up of the camshaft. Backlash and shaft wind-up can be avoided through an appropriate design of the cam-follower system. The speed variation due to load variations can be eliminated through an auxiliary torque bal-

ancing mechanism [13], [5]. A more classical approach consists of mounting an appropriately sized flywheel on the camshaft [12]. However, a flywheel cannot entirely suppress the speed variation, especially when its size is limited in order to ensure a good start/stop behaviour. This paper presents a cam design method that explicitly takes into account the speed variation due to (inertial) load variations, without trying to suppress it.

The concept of using variable speeds in cam-follower design has seldom been studied in literature. Rothbart [14] indicates the potentialities of using variable-speed cams, and designs a variable-speed cam mechanism in which the variable speed is delivered by a Withworth quick-return mechanism. Yan et al. [20] synthesize cams in the classical way through direct transformation of the desired follower displacement, but then optimize a polynomially parameterized cam input speed in order to reduce the peak values of the follower-output motion curves. Hsu and Chen [7] use a similar polynomial cam input speed but their optimization criterion is the minimization of the inertial part of the camshaft torque<sup>2</sup>. They obtain reductions of about 45% whereas the design method presented in this paper proves that the inertial part of the camshaft torque can be reduced to zero. Liu [11] proposes a systematic procedure using a finite element method to synthesize and analyze a high-speed cam-actuated elastic linkage with its actuator, a DC motor. This method takes into account the fluctuation of the speed of the driving cam and yields a cam that compensates for the entire machine dynamics at a single design speed. The method presented in this paper yields cams that only compensate for the inertial dynamics of a rigid cam-follower system, but they do so for any design speed. Furthermore they can be designed in a very simple way: no finite elements are needed, nor a model of the driving actuator, nor an accurate estimate of the viscous friction.

Section II introduces dimensionless trajectories as a way to keep the theoretical results as generally valid as possible. Section III gives the theoretical background of the design procedure, which makes clear that there is only one

<sup>1</sup>The optimal control technique is applicable to nonlinear models, while the Lagrange multiplier method and other linear techniques are not.

<sup>2</sup>i.e. the torque on the camshaft, required to accelerate and decelerate the follower inertia.

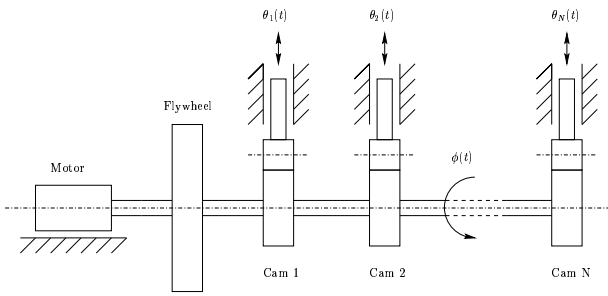


Fig. 1. Schematic representation of a cam-follower system with multiple followers. In this case the followers are translating.

design choice to be made, i.e. the value of the dimensionless coefficient of camshaft speed fluctuation  $\delta$ . Section IV investigates the influence of  $\delta$  on the (equivalent) camshaft inertia and the cam properties for a design example. For the same design example, section V compares (on simulation) the difference between the classical design procedure and the design procedure proposed in this paper.

## II. PROPERTIES OF DIMENSIONLESS TRAJECTORIES

### A. Dimensionless Follower Trajectories

Figure 1 schematically represents a cam-follower system with one camshaft and multiple followers. The periodic motion of the followers is described by their (translational or rotational) displacement  $\theta_i(t)$  as a function of time. Since the follower motions are periodic with period  $T$ , the functions  $\theta_i(t)$  have the following property:  $\theta_i(t + T) = \theta_i(t), \forall t, i$ . The index  $i$  refers to the  $i$ -th follower.

Using dimensionless parameters is a well known way [1], [2] to decouple the motion shape from the motion amplitude  $\Theta_i$  and the period of motion  $T$ :

$$\theta_i(t) = \Theta_i \cdot f_i\left(\frac{t}{T}\right) = \Theta_i \cdot f_i(\tau). \quad (1)$$

$\Theta_i$  has the dimension of [m] in the case of a translational follower and the dimension of [rad] in the case of a rotational follower.  $\tau = \frac{t}{T}$  is the dimensionless time. Since all displacements are periodic with period  $T$ , it is sufficient to consider time values  $t \in [0, T]$  or thus dimensionless time values  $\tau \in [0, 1]$ .  $f_i(\tau) : [0, 1] \rightarrow [0, 1]$  is the dimensionless displacement of the  $i$ -th follower, representing the shape of the follower motion. Since the functions  $\theta_i(t)$  are periodic with period  $T$ , the shape functions  $f_i(\tau)$  are periodic with period 1, which means that  $f_i(\tau) = f_i(\tau + 1), \forall \tau, i$ .

Applying the chain rule for differentiation to equation (1) yields the following proportional relations between the time derivatives of  $\theta_i(t)$  and the derivatives of  $f_i(\tau)$  with respect to  $\tau$ :

$$\frac{d^n \theta_i(t)}{dt^n} = \frac{\Theta_i}{T^n} \cdot f_i^{(n)}(\tau). \quad (2)$$

### B. Dimensionless Camshaft Trajectories

The motion of the camshaft is described by its rotation angle  $\phi(t)$  as a function of time. A possible way of using

dimensionless parameters is given by the following formula:

$$\phi(t) = 2\pi \cdot g\left(\frac{t}{T}\right) = 2\pi \cdot g(\tau). \quad (3)$$

Again,  $\tau \in [0, 1]$  is the dimensionless time, and  $g(\tau) : [0, 1] \rightarrow [0, g_{max} = 1]$  is the dimensionless camshaft displacement, representing the shape of the camshaft motion.  $g_{max}$  equals 1 since  $g_{max}$  equals  $g(\tau = 1)^3$  and  $g(\tau = 1)$  equals 1<sup>4</sup>. This definition of  $g(\tau)$  has the nice properties that (i) it is very similar to the definition of the functions  $f_i(\tau)$  and (ii) it yields a function  $g(\tau) : [0, 1] \rightarrow [0, 1]$ . However, it is not very suited for design. For design, it is better to use the dimensionless camshaft displacement  $h(\tau)$ , defined as [18]:

$$\phi(t) = 2\pi \cdot \sqrt{\frac{J_{ref}}{J_0}} \cdot h\left(\frac{t}{T}\right) = 2\pi \cdot \sqrt{\frac{J_{ref}}{J_0}} \cdot h(\tau). \quad (4)$$

Again,  $\tau \in [0, 1]$  is the dimensionless time, and  $h(\tau) : [0, 1] \rightarrow [0, h_{max}]$  is the dimensionless camshaft displacement, representing the shape of the camshaft motion, with  $h_{max} = h(\tau = 1)$  not necessarily equal to one.  $J_{ref}$  is a reference inertia equal to 1 kg-m<sup>2</sup>;  $J_0$  is the equivalent camshaft (rotational) inertia, including the motor inertia, the flywheel inertia, the camshaft inertia and the inertia of the cams.

Applying the chain rule for differentiation to equation (4) yields the following proportional relations between the time derivatives of  $\phi(t)$  and the derivatives of  $h(\tau)$  with respect to  $\tau$ :

$$\frac{d^n \phi(t)}{dt^n} = \frac{2\pi}{T^n} \cdot \sqrt{\frac{J_{ref}}{J_0}} \cdot h^{(n)}(\tau). \quad (5)$$

## III. DESIGN PROCEDURE: THEORETICAL BACKGROUND

The basis of the design procedure, is the assumption of a conservative system, which allows to calculate the camshaft speed based on the conservation of energy, as explained in section III-A. Section III-B introduces the dimensionless coefficient  $\delta$  as a way of making a well-founded choice of the initial camshaft speed. Section III-C proves that  $\delta$  fixes the value of the equivalent camshaft inertia  $J_0$ , whereas section III-D indicates how to calculate the cam motion laws. Both  $J_0$  and the cam motion laws are proven to be independent of the period of motion  $T$ .

### A. Camshaft Speed of a Conservative, Purely Inertial System

When friction is negligible, and no external motor acts on the cam-follower system, it is conservative. Hence, its total (kinetic and potential) energy remains constant and equal to the energy  $E_0$  at the start of the motion cycle:  $E(t) = E_0$ .

<sup>3</sup> $g(\tau)$  is a monotonically increasing function since  $g'(\tau)$  is always bigger than zero. This has as a consequence that  $g_{max} = g(\tau = 1)$ .

<sup>4</sup> $g(\tau = 1)$  equals 1, since the camshaft has to make one complete revolution during one period of motion:  $\phi(t = T) = 2\pi$ .

This paper considers a special class of conservative systems, i.e. systems where all forces are inertial. These systems are quite important in practice since inertial forces are often dominating, due to the tendency to increase the drive speed. In rigid, purely inertial systems, the potential energy equals zero, and the energy equation reduces to:  $E_{kin}(t) = E_{kin,0}$ . Applying the well-known expression for kinetic energy yields:

$$\frac{J_0 \cdot \dot{\phi}^2(t)}{2} + \sum_{i=1}^N \frac{J_i \cdot \dot{\theta}_i^2(t)}{2} = \frac{J_0 \cdot \dot{\phi}_0^2}{2} + \sum_{i=1}^N \frac{J_i \cdot \dot{\theta}_{i,0}^2}{2}. \quad (6)$$

$\dot{\phi}_0^2$  and  $\dot{\theta}_{i,0}^2$  are the initial values of  $\dot{\phi}(t)$  and  $\dot{\theta}_i(t)$  respectively.  $J_i$  is the inertia (rotational or translational) of the  $i$ -th follower, and  $N$  is the number of followers.

Based on (6), this section shows that, for this special class of conservative, purely inertial cam-follower systems, the motions and the inertias of the individual followers determine the dimensionless camshaft speed  $h'(\tau)$  in a unique way. Applying equations (5) and (2), substituting  $\Sigma \triangleq \frac{J_{ref}}{2} \cdot \frac{(2\pi)^2}{T^2}$  and substituting the dimensionless coefficients  $\zeta_i \triangleq \frac{J_i}{J_{ref}} \cdot \frac{\Theta_i^2}{(2\pi)^2}$ , yields:

$$\Sigma \cdot \left( h'^2(\tau) + \sum_{i=1}^N \zeta_i \cdot f_i'^2(\tau) \right) = \Sigma \left( h_0'^2 + \sum_{i=1}^N \zeta_i \cdot f_{i,0}'^2 \right),$$

or thus:

$$h'^2(\tau) + \sum_{i=1}^N \zeta_i \cdot f_i'^2(\tau) = h_0'^2 + \sum_{i=1}^N \zeta_i \cdot f_{i,0}'^2, \quad (7)$$

which expresses the conservation of kinetic energy in a dimensionless way. Since  $\Sigma = \frac{J_{ref}}{2} \cdot \frac{(2\pi)^2}{T^2}$  has the dimension of kinetic energy, the left part of (7) is defined as the dimensionless kinetic energy  $\epsilon(\tau)$ :

$$\epsilon(\tau) = \frac{E_{kin}(\tau \cdot T)}{\Sigma} = \underbrace{h'^2(\tau)}_{\epsilon_{mot}(\tau)} + \underbrace{\sum_{i=1}^N \zeta_i \cdot f_i'^2(\tau)}_{\epsilon_{fol}(\tau)}. \quad (8)$$

$\epsilon_{fol}(\tau)$ , the dimensionless kinetic energy of the followers, is dependent on the  $N$  motion shapes  $f_i'(\tau)$ , the  $N$  motion amplitudes  $\Theta_i$  and the  $N$  follower inertias  $J_i$ . It is however not dependent on the period of motion  $T$ .

Based on (7),  $h'(\tau)$  can be calculated as:

$$h'(\tau) = \sqrt{h_0'^2 + \sum_{i=1}^N \zeta_i \cdot f_{i,0}'^2 - \sum_{i=1}^N \zeta_i \cdot f_i'^2(\tau)} \quad (9)$$

$$= \sqrt{\epsilon_{mot,0} + \epsilon_{fol,0} - \epsilon_{fol}(\tau)}. \quad (10)$$

Equation (10) allows to draw four important conclusions.

- $h'(\tau)$  is dependent on  $\epsilon_{mot,0}$ ,  $\epsilon_{fol,0}$  and  $\epsilon_{fol}(\tau)$ . However, when the  $N$  motion shapes  $f_i(\tau)$ , the  $N$  motion amplitudes  $\Theta_i$  and the  $N$  follower inertias  $J_i$  are given (as is normally the case),  $\epsilon_{fol}(\tau)$  and  $\epsilon_{fol,0}$  are entirely determined and

there remains one basic design choice to be made: the value of  $\epsilon_{mot,0} = h_0'^2$ .

- $h'(\tau)$  is independent of  $T$ , since  $\epsilon_{fol}(\tau)$  is.
- Limiting the frequency content of the motion shapes  $f_i'(\tau)$  doesn't limit the frequency content of  $h'(\tau)$  because of the nonlinear square root operation.
- $h'(\tau)$  can be calculated without any information concerning the cam profiles, and without the need of time integration.

### B. Choice of the Initial Camshaft Speed value

In order to make a well-founded choice of  $h'_0$ , a dimensionless coefficient of motor speed fluctuation  $\delta$  is introduced:

$$\delta = \frac{\dot{\phi}_{min}}{\dot{\phi}_{max}} = \frac{\frac{2\pi}{T} \cdot \sqrt{\frac{J_{ref}}{J_0}} \cdot h'_{min}}{\frac{2\pi}{T} \cdot \sqrt{\frac{J_{ref}}{J_0}} \cdot h'_{max}} = \frac{h'_{min}}{h'_{max}}. \quad (11)$$

The relationship between  $\delta$  and  $h'_0$  is derived as follows. Substituting  $\epsilon_{mot,0} = h_0'^2$  into equation (10) yields:

$$h'^2(\tau) = h_0'^2 + \epsilon_{fol,0} - \epsilon_{fol}(\tau). \quad (12)$$

Consequently it is easy to see that:

$$h_{min}'^2 = h_0'^2 + \epsilon_{fol,0} - \epsilon_{fol,max} \quad (13)$$

$$h_{max}'^2 = h_0'^2 + \epsilon_{fol,0} - \epsilon_{fol,min}. \quad (14)$$

Substituting (13) and (14) into (11) and solving  $h'_0$  from the resulting equation yields the following relationship between  $h'_0$  and  $\delta$ :

$$h_0'^2 = -\epsilon_{fol,0} + \frac{\epsilon_{fol,max} - \delta^2 \cdot \epsilon_{fol,min}}{1 - \delta^2}. \quad (15)$$

This equation can be simplified by choosing the time instant where the kinetic energy of the followers is minimal, as the beginning of the motion cycle:  $\epsilon_{fol,0} = \epsilon_{fol,min}$ . This doesn't compromise the generality of the equations: it's just a matter of convention<sup>5</sup>. Consequently (15) reduces to:

$$h_0'^2 = \frac{\epsilon_{fol,max} - \epsilon_{fol,min}}{1 - \delta^2}. \quad (16)$$

This equation shows that  $h'_0$  is dependent on: (i) the chosen value of  $\delta$  and (ii)  $\epsilon_{fol}(\tau)$ . Hence,  $h'_0$  is independent of  $T$ . As  $\epsilon_{fol,max}$  is always bigger than  $\epsilon_{fol,min}$ , and  $\delta$  is always smaller than one,  $h'_0$  will always be a real number.

### C. Calculation of the Equivalent Camshaft Inertia $J_0$

The assumption that the system is conservative, yields that  $J_0$  cannot be freely chosen. This can be understood by taking the average of both sides of equation (5) for  $n = 1$ , which yields:

$$\dot{\phi}_{ave} = \frac{2\pi}{T} \cdot \sqrt{\frac{J_{ref}}{J_0}} \cdot h'_{ave}.$$

<sup>5</sup>For a system with one follower, this convention boils down to choosing the instant where the follower stands still, as the beginning of the motion cycle.

Since  $\dot{\phi}_{ave}$ , the average camshaft speed, must equal  $\frac{2\pi}{T}$ , the following constraint is imposed on  $J_0$ :

$$J_0 = J_{ref} \cdot h_{ave}'^2, \quad (17)$$

with  $h_{ave}'$  the average value of  $h'(\tau)$  over the interval  $[0, 1]$ .  $J_0$  is independent of  $T$ , since  $h'(\tau)$  is independent of  $T$ .

#### D. Calculation of the Cam Motion Law

This section proves that not only  $J_0$ , but the cams as well, are independent of  $T$ , by showing that the cam motion law  $F_i(\phi)$  is independent of  $T$ . The cam motion law  $F_i(\phi)$  gives the  $i$ -th follower displacement  $\theta_i$  as a function of the cam angle  $\phi$ :  $\theta_i = F_i(\phi)$ .  $F_i(\phi)$  is defined by the look-up table with  $\phi(t)$  as inputs and  $F_i(\phi(t)) = \theta_i(t)$  as outputs. In order to prove that  $F_i(\phi)$  is independent of  $T$ , it is sufficient to prove that both the entries  $\phi(t)$  and the corresponding values  $F_i(\phi(t)) = \theta_i(t)$  of the look-up table are independent of  $T$ . Since

$$\phi(t) = 2\pi \cdot \sqrt{\frac{J_{ref}}{J_0}} \cdot h(\tau),$$

and  $h(\tau)$  and  $J_0$  are independent<sup>6</sup> of  $T$ ,  $\phi(t)$  is independent of  $T$ . On the other hand  $\theta_i(t) = \Theta_i \cdot f_i(\tau)$  is independent of  $T$  by definition of  $f_i(\tau)$ .

The motion law  $F_i(\phi)$  itself doesn't contain any information about the character of the drive speed, i.e. it gives for each camshaft angle  $\phi$  a corresponding displacement  $\theta_i = F_i(\phi)$ , without saying anything about the time trajectory of  $\phi(t)$ . Consequently, from the moment the motion law  $F_i(\phi)$  is determined, the design procedures for a cam with constant drive speed and for a cam with variable drive speed are exactly the same.

#### E. Design Procedure

As a summary of the previous sections, this section formulates a design procedure that consists of seven steps and starts from the following data: the  $N$  follower motions  $\theta_i(t)$  and the  $N$  follower inertias  $J_i$ :

1. Calculate  $f_i'(\tau)$  according to (2), and  $\zeta_i = \frac{J_i}{J_{ref}} \cdot \frac{\Theta_i^2}{(2\pi)^2}$ .
2. Calculate  $\epsilon_{fol}(\tau) = \sum_{i=1}^N \zeta_i \cdot f_i'^2(\tau)$ . Determine the value of  $\tau$  for which  $\epsilon_{fol}(\tau)$  is minimal. This  $\tau$ -value becomes the (new) beginning of the motion cycle.
3. Choose a value of  $\delta = \frac{\phi_{min}}{\phi_{max}}$ . This choice determines the value of  $h_0'$  according to (16).
4. Calculate  $h'(\tau)$  according to (9). Calculate  $h(\tau)$  by analytically integrating  $h'(\tau)$  [17]. The integration constant is chosen such that  $h(0) = 0$ .
5. Calculate the value of  $J_0$  according to (17).
6. Calculate the motion law  $F_i(\phi)$  as follows.  $\theta_i(t) = F_i(\phi(t))$  is given, and  $\phi(t)$  is obtained from  $h(\tau)$  by applying (4).  $F_i(\phi)$  is then defined by the look-up table with  $\phi(t)$  as inputs and  $\theta_i(t) = F_i(\phi(t))$  as outputs.

<sup>6</sup> $h(\tau)$  is obtained by analytically integrating [17]  $h'(\tau)$  with respect to  $\tau$ ; since  $h'(\tau)$  is independent of  $T$ ,  $h(\tau)$  is independent of  $T$  too.

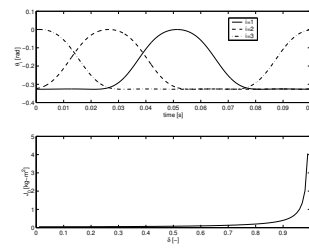


Fig. 2. The desired displacement  $\theta_i(t)$  as a function of time for the three followers of the design example (upper figure), and the value of  $J_0$  as a function of  $\delta$  (lower figure).

7. To determine the cam profiles, the design procedure has to take into account the type of the cam and the follower (e.g. linear or rotary follower). The algorithms for calculating the cam profile based on the knowledge of  $F(\phi)$  and the type of cam-follower configuration are well known [2].

This design approach yields cams that are compensated for the inertial dynamics, since the motor torque required to drive the cam-follower system is equal to zero (and the only forces in the system are inertial forces).

#### IV. DESIGN EXAMPLE: INFLUENCE OF $\delta$

This section investigates the influence of the value of  $\delta$  on (i)  $J_0$  and (ii) the cams of a cam-follower system with three followers ( $N = 3$ ). Each of the three cam-follower configurations consists of a rotating, conjugate cam with an oscillating follower, having an inertia  $J_i$  of 0.3758 kg-m<sup>2</sup>. The upper figure of figure 2 shows one period ( $T = 0.1$ s) of the desired displacement  $\theta_i(t)$  as a function of time for the three followers.

The lower figure of figure 2 shows that the value of  $J_0$  increases a function of  $\delta$ : a slow increase for values of  $\delta$  up to 0.8 but a very rapid increase for higher values of  $\delta$ .

Figure 3 shows, for the slave cam of the first cam-follower configuration ( $i = 1$ ), how the cam profile and the cam properties change as a function of  $\delta$ . The upper part of the cam profile completely degenerates for values of  $\delta$  smaller than 0.5. This can be explained by the fact that the cam motion law becomes very pointed for small values of  $\delta$ . The degeneration of the cam profile for small values of  $\delta$  is confirmed by the deterioration of the cam properties. The maximal pressure angle  $\alpha_{max}$ , shown in the upper left figure, becomes much too big for  $\delta \in [0.4, 1]$ , though it has reasonable values (i.e. values lower than 20°) for higher  $\delta$ -values. Consequently, the maximal Hertzian pressure  $\sigma_{H,max}$  on the cam profile, shown in the lower left figure, has reasonable values for  $\delta$  higher than 0.6, but rapidly increases for smaller values of  $\delta$ .

The degeneration of the cam profile can also be derived from the upper middle figure, which shows the minimal positive value of the radius of curvature  $\rho$ . This minimal value should be greater than the radius  $r_{fol} = 0.05$ m of the roller follower, in order to avoid *underrolling*. Only positive values of  $\rho$  should be considered since only convex parts of a cam profile can exhibit underrolling. The 0.05m-limit is indicated with a dashed line. The figure shows that for  $\delta$

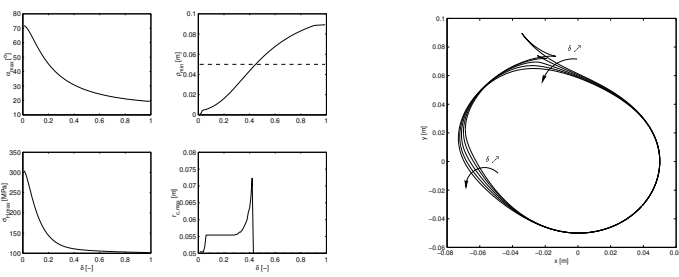


Fig. 3. The properties of the slave cam of the first cam-follower configuration ( $i = 1$ ) as a function of  $\delta$ : maximal pressure angle (upper left figure), minimal positive radius of curvature (upper middle figure), maximal Hertzian pressure (lower left figure), maximal cutter radius (lower middle figure) and cam profile (right figure). The cam profile is shown for five different values of  $\delta$ , i.e  $\delta = 0.1$ ,  $\delta = 0.3$ ,  $\delta = 0.5$ ,  $\delta = 0.7$  and  $\delta = 0.9$ . The arrows indicate increasing values of  $\delta$ .

smaller than  $\pm 0.4$ , the slave cam exhibits underrolling.

The concave parts of a cam profile cannot exhibit underrolling but there is another possible problem there, i.e. *undercutting*, which means that the radius of the cutter, used for creating the cam profile, is too big to mill the cam profile. The lower middle figure shows the maximal value of the cutter radius  $\rho_{c,max}$  in order to avoid undercutting. For values of  $\delta$  to the right of the peak in the diagram, no value of  $\rho_{c,max}$  is shown, since for these values of  $\delta$ , there are no concave parts on the cam profile, and hence no danger of undercutting.

As a conclusion, it can be stated that the value of  $\delta$  is a compromise between obtaining a small  $J_0$  (a small flywheel) and maintaining good cam properties. For this design example, a value of  $\delta \approx 0.7$  seems to be a good compromise:  $J_0$  remains reasonably small, the pressure angle and the normal force have limited values, there is no underrolling and no limitation on the cutter radius since the cam has no concave parts.

## V. DESIGN EXAMPLE: COMPARISON BETWEEN A CONSTANT AND A VARIABLE DRIVE SPEED

This section compares (on simulation) the behaviour of a cam-follower system with cams that are designed in two different ways: (i) cams designed in the traditional way, for a constant drive speed (the cam-follower system with these cams is called the CON-system) and (ii) cams designed for a variable drive speed, with  $\delta = 0.9^7$  (the cam-follower system with these cams is called the VAR-system). For both the CON- and the VAR-system, the follower motions  $\theta_i(t)$  and follower inertias  $J_i$  are the same as in the design example of the previous section. Both systems are driven with an identical permanent magnet DC-motor<sup>8</sup> with a classically designed feedback control system.

There is viscous friction between the camshaft and the environment, quantified by  $b$  [N-m/(rad/s)], the coefficient of viscous friction. Both the CON- and the VAR-system

are simulated for three different values of  $b$ :  $b = 0$ ,  $b = 2.5$  and  $b = 25$ . For  $b = 2.5$ , the energy dissipation  $E_{dissip}$  during one motion cycle approximately equals 1 kJ; for  $b = 25$ , the energy dissipation is ten times bigger. These values should be compared with the total kinetic energy of the system, which approximately equals 33 kJ. When  $b = 0$ , there is no friction in the system, as assumed in the design procedure. Consequently, in the VAR-system, the required motor torque should be zero, since the cams are compensated for the inertial dynamics. Furthermore, the desired and actually realized camshaft motion and follower motions should coincide. The discussion hereafter shows that this is approximately true.

The upper figure in figure 4 compares the desired camshaft speed  $\dot{\phi}_{des}(t)$  and the actually realized camshaft speed  $\dot{\phi}_{act}(t)$  for the CON- and the VAR-system. For the CON-system,  $\dot{\phi}_{des}(t)$  (equal to 62.83 rad/s over the whole period) and  $\dot{\phi}_{act}(t)$  do not coincide at all, in contrary to the VAR-system where the difference between them is very small, at least for  $b = 0$  and  $b = 2.5$ . Only for  $b = 25$ , the difference is visible.

The good correspondence between  $\dot{\phi}_{des}(t)$  and  $\dot{\phi}_{act}(t)$  in the VAR-system yields three important advantages. First of all, the required motor torque is much lower than in the CON-system, since the error signal provided to the controller is very small. This can be clearly seen in the lower figure of figure 4. In the VAR-system,  $T_{mot,max}$  is 0.08 N-m (theoretically zero) for  $b=0$ , 18 N-m for  $b=2.5$  and 155 N-m for  $b=25$ , which is much smaller than  $T_{mot,max} \approx 400$  N-m in the CON-system. The difference in motor torque between the CON- and the VAR-system can be understood by noticing that in the CON-system, the motor has to compensate the friction force and the inertial forces, while in the VAR-system, the motor has to compensate nothing but the viscous friction force, since its cams are compensated for the inertial dynamics.

A second advantage is the more accurate realization of the follower motions. Table 1 gives the relative error [%] between the amplitudes of the first six harmonics of the actually realized position and the desired position of the first follower. In the VAR-system, these relative errors are very small for  $b=0$  (theoretically zero) and  $b=2.5$  and reasonable for  $b=25$ . For the CON-system, however, these relative errors are considerably higher, especially for the higher order harmonics. Notice though that the (desired) amplitude of these higher harmonics is very small.

A third advantage is the fact that in the VAR-system, the  $\dot{\phi}_{act}(t)$  spectrum can be robustly predicted by calculating the  $\dot{\phi}_{des}(t)$  spectrum, since the difference between  $\dot{\phi}_{act}(t)$  and  $\dot{\phi}_{des}(t)$  remains small, even for high values of  $b$ . Calculating the spectrum of  $\dot{\phi}_{des}(t)$  has the advantage of (i) being very easy since it requires no time simulation and (ii) not requiring any information concerning the actuator or the controller. In the CON-system however, the calculation of the  $\dot{\phi}_{act}(t)$  spectrum requires a time simulation of the entire system (including the actuator and the controller). This third advantage may be important in an early design stage, where the designer may not yet know

<sup>7</sup>This value fixes the value of  $J_0$  in the VAR-system. The value of  $J_0$  in the CON-system is taken equal to this value.

<sup>8</sup>No saturation is taken into account, which means that the DC-motor can deliver a torque that can be arbitrarily large.

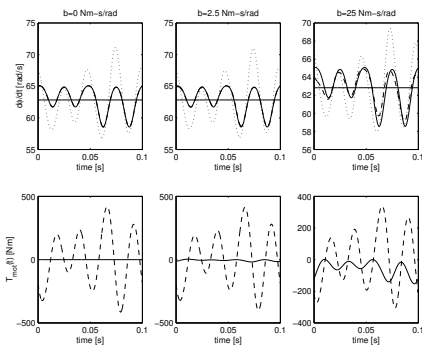


Fig. 4. Upper figure: comparison of  $\dot{\phi}_{des}(t)$  for the VAR-system (full line), with  $\phi_{act}(t)$  in the VAR-system (dashed line) and in the CON-system (dotted line), for three values of  $b$ . Lower figure: comparison of the required motor torque in the VAR-system (full line) and in the CON-system (dashed line), for three values of  $b$ .

the type of actuator or controller but still wants to have an idea of the spectrum of the camshaft motion in order to avoid the excitation of structural resonances.

## VI. CONCLUSION

A design method for rigid cam-follower systems with dominating inertial forces has been developed. The method is based on the assumption of a conservative, purely inertial system, and has only one design parameter: the amount of camshaft speed variation  $\delta$ .  $\delta$  fixes the value of the camshaft inertia (and thus the size of the flywheel), independently of the period of motion  $T$ . The cams designed in this way compensate for the inertial dynamics for any period of motion.

The value of  $\delta$  is a compromise between obtaining a small flywheel and keeping the cam properties reasonably good (e.g.  $\delta \approx 0.7$ ). The comparison between a system with variable desired camshaft speed and a system with constant desired camshaft speed has shown that this new way of designing cams has the following advantages, even for non-conservative, non-purely inertial cam-follower systems: (i) more accurate follower motions, (ii) lower motor torques and (iii) a camshaft motion spectrum that is easily and robustly predictable.

## Acknowledgment

Bram Demeulenaere is research assistant with the Fund for Scientific Research–Flanders (Belgium) (F.W.O.). This work also benefits from the Belgian Inter-University Poles of Attraction Programme, initiated by the Belgian State, Prime Minister’s Office, Science Policy Programming. K. U. Leuven’s Concerted Research Action GOA/99/04 is gratefully acknowledged. The scientific responsibility is assumed by its authors.

## REFERENCES

- [1] J. Angeles and C. López-Cajún. *Optimization of Cam Mechanisms*. Kluwer Academic Publishers, 1991.
- [2] F. Y. Chen. *Mechanics and Design of Cam Mechanisms*. Pergamon Press, 1982.
- [3] M. Chew and C. H. Chuang. Minimizing residual vibrations in high-speed cam-follower systems over a range of speeds. *Transac-*

	DES	VAR-system			CON-system		
		$b = 0$	$b = 2.5$	$b = 25$	$b = 0$	$b = 2.5$	$b = 25$
1	0,076	0,0001	-0,06	-0,4	0,2	0,3	0,6
2	0,039	0,0002	0,07	0,3	2,1	2,0	1,2
3	0,009	0,0005	0,52	2,7	8,2	7,4	2,4
4	0,003	0,0010	-0,54	-3,7	4,1	5,0	8,9
5	0,003	0,0029	0,19	-1,0	30,3	29,8	23,0
6	0,001	0,0093	0,60	-4,7	88,7	90,5	58,0

Table 1: The relative error [%] on the amplitudes of the first six harmonics of the displacement of the first follower. The second column gives the desired amplitudes, the next three columns give the relative error for the VAR-system and the last three columns give the relative error for the CON-system. For both the VAR and the CON-system, three values of  $b$  (0, 2.5 and 25) are compared.

- tions of the ASME, Journal of Mechanical Design*, 117:166–172, 1995.
- [4] M. Chew, F. Freudenstein, and R. W. Longman. Application of optimal control theory to the synthesis of high-speed cam-follower systems, part 1: Optimality criteria, part 2: System optimization. *Transactions of the ASME, Journal of Mechanisms, Transmissions, and Automation in Design*, 105:576–591, 1993.
- [5] D. B. Dooner. Use of noncircular gears to reduce torque and speed fluctuations in rotating shafts. *Transactions of the ASME, Journal of Mechanical Design*, 119:299–306, 1997.
- [6] B. C. Fabien, R. W. Longman, and F. Freudenstein. The design of high-speed dwell-rise-dwell tuned cam displacement curves using linear quadratic optimal control theory. *Transactions of the ASME, Journal of Mechanical Design*, 116:867–874, 1994.
- [7] Meng-Hui Hsu and Wei-Ren Chen. On the design of speed functions for improving torque characteristics of cam-follower systems. *Proc. 10th World Congress on the Theory of Machine and Mechanisms*, pages 272–277, 1999. Oulu, Finland.
- [8] K. Kanzaki and K. Itao. Polydyne cam mechanisms for typehead positioning. *Transactions of the ASME, Journal of Engineering for Industry*, 94:250–254, 1972.
- [9] M. P. Koster. Effect of flexibility of driving shaft on the dynamic behavior of a cam mechanism. *Transactions of the ASME, Journal of Engineering for Industry*, pages 595–602, May 1975.
- [10] H. Kwakernaak and J. Smit. Minimum vibration cam profiles. *J. of Mech. Engr. Sci.*, 10:219–227, 1968.
- [11] Hsin-Ting J. Liu. Synthesis and steady-state analysis of high-speed elastic cam-actuated linkages with fluctuated speeds by a finite element method. *Transactions of the ASME, Journal of Mechanical Design*, 119:395–402, 1997.
- [12] H. H. Mabie and C. F. Reinholtz. *Mechanisms and Dynamics of Machinery*. Wiley, 1987.
- [13] M. Nishioka. State of the art of torque compensation cam mechanisms. *Proc. 9th World Congress on the Theory of Machine and Mechanisms*, pages 713–717, 1995. Milan, Italy.
- [14] H. A. Rothbart. *Cams–Design, Dynamics, and Accuracy*. Wiley, 1956.
- [15] L. N. Srinivasan and Q. Jeffrey Ge. Designing dynamically compensated and robust cam profiles with bernstein-bézier harmonic curves. *Transactions of the ASME, Journal of Mechanical Design*, 120:40–45, 1998.
- [16] D. A. Stoddart. Polydyne cam design. *Machine Design*, pages January, 121–135; February, 146–154; March, 149–164, 1953.
- [17] J. Swevers, C. Ganseman, D. Tükel, J. De Schutter, and H. Van Brussel. Optimal robot excitation and identification. *IEEE Transactions on Robotics and Automation*, 13:730–739, 1997.
- [18] H. J. Van de Straete and J. De Schutter. Optimal variable transmission ratio and trajectory for an inertial load with respect to servo motor size. *Transactions of the ASME, Journal of Mechanical Design*, 121:544–551, 1999.
- [19] J. L. Wiederrich and B. Roth. Dynamic synthesis of tuned cam displacement curves using finite trigonometric series. *Transactions of the ASME, Journal of Engineering for Industry*, pages 287–293, Feb. 1975.
- [20] Hong-Sen Yan, Mi-Ching Tsai, and Meng-Hui Hsu. A variable-speed method for improving motion characteristics of cam-follower systems. *Transactions of the ASME, Journal of Mechanical Design*, 118:250–258, 1999.